This article was downloaded by: [National Chiao Tung University 國立交通大學]
On: 24 April 2014, At: 22:44
Publisher: Taylor & Francis
Informa Ltd Registered in England and Wales Registered Number: 1072954 Registered office: Mortimer House, 37-41 Mortimer Street, London W1T 3JH, UK

Aerosol Science and Technology
Publication details, including instructions for authors and subscription information:
http://www.tandfonline.com/loi/uast20

Enhancement of Extrinsic Charging Efficiency of a Nanoparticle Charger with Multiple Discharging Wires

Chuen-Jinn Tsai [a] , Guan-Yu Lin [a] , Hui-Lin Chen [a] , Cheng-Hsiung Huang [b] & Manuel Alonso [c]
[a] Institute of Environmental Engineering, National Chiao Tung University , Hsin Chu, Taiwan
[b] Department of Environmental Engineering and Health , Yuanpei University , Hsin Chu, Taiwan
[c] National Center for Metallurgical Research (CSIC) , Madrid, Spain
Published online: 28 Jul 2010.

To cite this article: Chuen-Jinn Tsai , Guan-Yu Lin , Hui-Lin Chen , Cheng-Hsiung Huang & Manuel Alonso (2010) Enhancement of Extrinsic Charging Efficiency of a Nanoparticle Charger with Multiple Discharging Wires, Aerosol Science and Technology, 44:10, 807-816, DOI: 10.1080/02786826.2010.492533

To link to this article: http://dx.doi.org/10.1080/02786826.2010.492533

PLEASE SCROLL DOWN FOR ARTICLE

Taylor & Francis makes every effort to ensure the accuracy of all the information (the "Content") contained in the publications on our platform. However, Taylor & Francis, our agents, and our licensors make no representations or warranties whatsoever as to the accuracy, completeness, or suitability for any purpose of the Content. Any opinions and views expressed in this publication are the opinions and views of the authors, and are not the views of or endorsed by Taylor & Francis. The accuracy of the Content should not be relied upon and should be independently verified with primary sources of information. Taylor and Francis shall not be liable for any losses, actions, claims, proceedings, demands, costs, expenses, damages, and other liabilities whatsoever or howsoever caused arising directly or indirectly in connection with, in relation to or arising out of the use of the Content.

This article may be used for research, teaching, and private study purposes. Any substantial or systematic reproduction, redistribution, reselling, loan, sub-licensing, systematic supply, or distribution in any form to anyone is expressly forbidden. Terms & Conditions of access and use can be found at http://www.tandfonline.com/page/terms-and-conditions

Aerosol Science and Technology, 44:807–816, 2010
Copyright © American Association for Aerosol Research
ISSN: 0278-6826 print / 1521-7388 online
DOI: 10.1080/02786826.2010.492533

Enhancement of Extrinsic Charging Efficiency of a Nanoparticle Charger with Multiple Discharging Wires

Chuen-Jinn Tsai,[1] Guan-Yu Lin,[1] Hui-Lin Chen,[1] Cheng-Hsiung Huang,[2] and Manuel Alonso[3]

[1]*Institute of Environmental Engineering, National Chiao Tung University, Hsin Chu, Taiwan*
[2]*Department of Environmental Engineering and Health, Yuanpei University, Hsin Chu, Taiwan*
[3]*National Center for Metallurgical Research (CSIC), Madrid, Spain*

Downloaded by [National Chiao Tung University] at 22:44 24 April 2014

A unipolar charger with multiple discharging wires has been developed and investigated to enhance the extrinsic charging efficiency of nanoparticles by using sheath air near the wall of the charger. The applied voltage of the charger ranged from +4.0 to +10 kV, corresponding to corona current from 0.02 to 119.63 μA. Monodisperse NaCl particles of 10 $\sim$ 50 nm and Ag particles of 2.5 $\sim$ 10 nm in diameter were produced to test the performance of the charger with multiple discharging wires and to investigate the particle loss at different sheath flow rates, corona voltages and sheath air velocities. Results showed that the optimal efficiency in the charger was obtained at +9 kV applied voltage, 10 L/min aerosol flow rate and 20 L/min sheath air flow rate. The extrinsic charging efficiency increased from 2.86% to 86.3% in the charger as the particle diameter increasing from 2.5 to 50 nm. The TDMA (tandem-differential mobility analyzer) technique was used to investigate the charge distribution, and the charge distributions in the exit were obtained at the optimal operating condition.

INTRODUCTION

The electrical behavior of aerosol particles is one of the most significant subjects in aerosol science from both fundamental studies and practical applications. Particle charging plays an important role in monitoring and measurement systems, such as an aerosol sizing tool, a differential mobility analyzer (DMA; Knutson and Whitby 1975), and the control of particles by using the electrostatic precipitator (Yoo et al. 1997; Huang et al. 2002). The former research found that it is difficult to charge ultrafine particles. As a result, a variety of aerosol charging methods have been developed and proposed in different applications, one of these research elements is nanoparticle charger.

Received 12 October 2009; accepted 4 May 2010.
The authors would like to thank the National Science Council of the Republic of China for financially supporting this research under Contract No. NSC 97-2923-E-264 -001-MY2.
Address correspondence to Cheng-Hsiung Huang, No. 306, Yuanpei St., Hsin Chu, 300, Taiwan. E-mail: chhuang@mail.ypu.edu.tw

Ion diffusion charging is usually used for ultrafine particles such as bipolar and unipolar charging. The procedure of charging particles in a bipolar ion environment, such as radioactive sources (Am-214; Kr-85; Po-210), have been widely used in characterization of particle size distribution. One example is the scanning mobility particle sizer (SMPS, TSI model 3080; Wang and Flagan 1990). There are charging and recharging by ions of opposite polarity happen at the same time, hence, the neutralizing causes low charging efficiency which is only about 4.4% positively charged and 5.6% negatively charged for 10 nm particles (TSI model 3077A; Reischl et al. 1996). The other researchers found unipolar charging which is more efficient than bipolar ions for charging nanoparticles. The varied unipolar charging methods are expected to achieve higher charging efficiency of nanoparticles. Experimental data of charging efficiency for nanoparticles under 10 nm have been reported by Buscher et al. (1994) using corona discharge and Wiedensohler et al. (1994), who used a radioactive source ^{224}Cm to generate bipolar ions in two boxes separated by central charging region and an alternative electric field to draw unipolar ions into charging zone. The AC electrical field moved charged particles in a zigzag manner, keeping them away from the wall of the charger and minimizing charged particle loss. However, in this design, the effect of AC field was less useful to charge particles efficiently and reduce loss. After that, other Hewitt type chargers were still proposed to reduce the charged particles loss (Kruis and Fissan 2001; Biskos et al. 2005). In these studies, the extrinsic charging efficiency achieved was about 30% for 10 nm positive charged particles in the study of the former, 25% and 60% for 10 nm and 20 nm positively charged particles in the research of the latter, respectively. However, Marquard et al. (2006a) concluded that chargers by using an AC field to bring ions colliding particles could not improve the compromise between the average charge and loss for ultrafine particles.

Since most bipolar chargers might have the low extrinsic charging efficiency due to charging and discharging mechanism. Chen and Pui (1999) designed a unipolar charger with the parallel configuration of aerosol flow and ion current. A

Downloaded by [National Chiao Tung University] at 22:44 24 April 2014

relatively weak electrical field was applied to keep the same polarity ions with aerosols and collect the opposite polarity ions from a ^{210}Po radioactive source. They implemented sheath air surrounding the aerosol flow to keep charged particles in a core region for avoiding electrostatic loss. Thus, the extrinsic charging efficiency was found as high as 22% for 3 nm positively charged particles based on flux efficiency. However, the use of radioactive material needs to consider the tight safety regulations and the relatively high cost. Charging aerosols with unipolar ions produced by corona discharging is therefore an alternative technique.

Hernandez-Sierra et al. (2003) proposed a corona charger of needle inside a tube. The corona discharge takes place around a sharp-point stainless steel electrode, and aerosols collide directly with unipolar ions. They demonstrated good performance of a corona ionizer in charging nanoparticle. Later on, Alonso et al. (2006) and Qi et al. (2008) changed the configuration of the corona charger designed by Hernandez-Sierra et al. (2003) to develop their chargers. Besides, the ion jet was injected into a chamber to mix with particles and the charger (Qi et al. 2007). The extrinsic charging efficiencies of nanoparticles were found to be similar to those of various corona chargers. Moreover, in the previous results (Tsai et al. 2008), a unipolar charger with multiple discharging wires was developed for increasing the aerosol flow rate and enhancing the charging efficiency of nanoparticles. Results showed that increasing the corona voltage resulted in a higher ion number concentration. However, the higher electrostatic loss occurred due to stronger electrical field strength. For example, there is 15% electrostatic loss and 10% diffusion loss for particles above 20 nm, and severe diffusion loss of 50% for 10 nm particles at 10 L/min aerosol flow and 9 L/min sheath flow for the discharging voltages from 5.4 to 6.8 KV. The extrinsic charging efficiency increased from 10.6% to 74.2% when the particle diameter was increased from 10 to 50 nm. The study also reported that the sheath air problem needs to be investigated further to reduce the particle loss in the charger.

In the present work, the particles with diameter of 2.5 $\sim$ 10 nm were produced further to evaluate the extrinsic charging efficiency of the charger with multiple discharging wires at different operating conditions. Since the sheath air flow is an important parameter on the reduction of charged particle loss and the enhancement of the extrinsic charging efficiency, the performance of the charger was tested at different sheath flow rates, corona voltages, and sheath air velocities. The charge distribution and mean charge of nanoparticles were also measured and compared with each other.

EXPERIMENTAL METHOD

Design of Unipolar Nanoparticle Chargers

Figure 1 shows the schematic diagram of the developed unipolar charger with multiple discharging wires. In this study, we reduce the gap between aluminum shroud and tube wall of the corona unipolar charger with multiple discharging wires to increase the sheath air velocity. The charger has an inner Teflon core to fix four gold wires of 25 μm in diameter and 26 mm in length. Due to the length of wires was too long to result in much charged particle loss, the Teflon tube was used to cover unnecessary length of wires. Hence, the effective length of the wires was cut down to 15 mm to reduce the possible particle loss and deposition. The space beneath the Teflon tube was filled by an aluminum cylinder which forms a simple geometry of central column to reduce the residence time of particles outside charging region and the possible diffusion loss of particles and to enhance the uniformity of ion production. The wires were operated at positive DC voltage and placed in axial symmetry to produce the uniform ion concentration. The outer stainless steel casing was grounded, so that positive ions are produced from the surface of the wires and move fast to the wall of charger. The annular space between the gold wires and the stainless steel casing where aerosol charging took place simultaneously is called the charging zone. In order to reduce charged particle loss in the charging zone due to strong electrical field which form in this space, a filtered sheath air flow was introduced to the charger from the 0.1 mm slit formed by the aluminum shroud and the outer casing. The other aluminum shroud was used to form 0.5 mm slit to test the charged particle loss in the charging zone at different sheath air velocities.

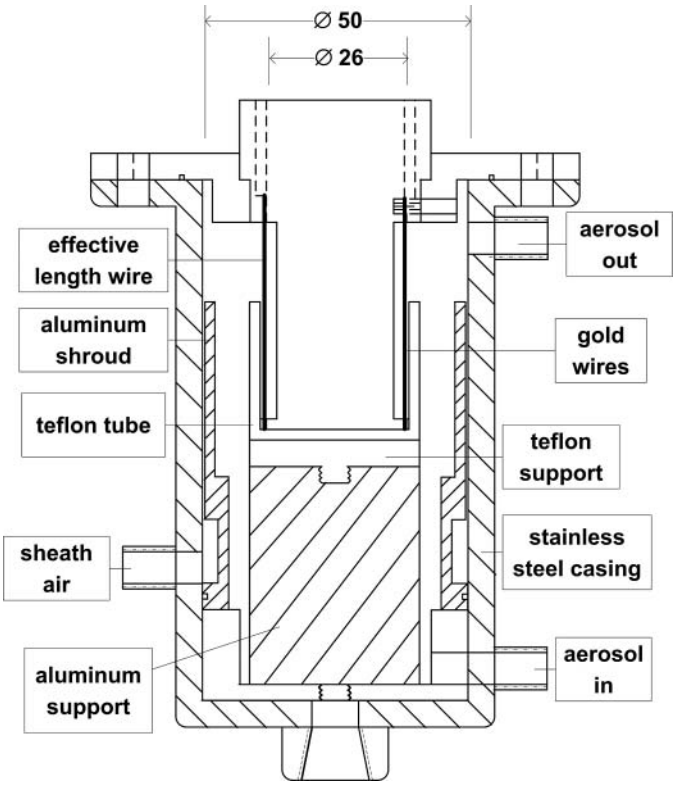

FIG. 1. Schematic diagram of present unipolar charger (unit: mm).

Downloaded by [National Chiao Tung University] at 22:44 24 April 2014

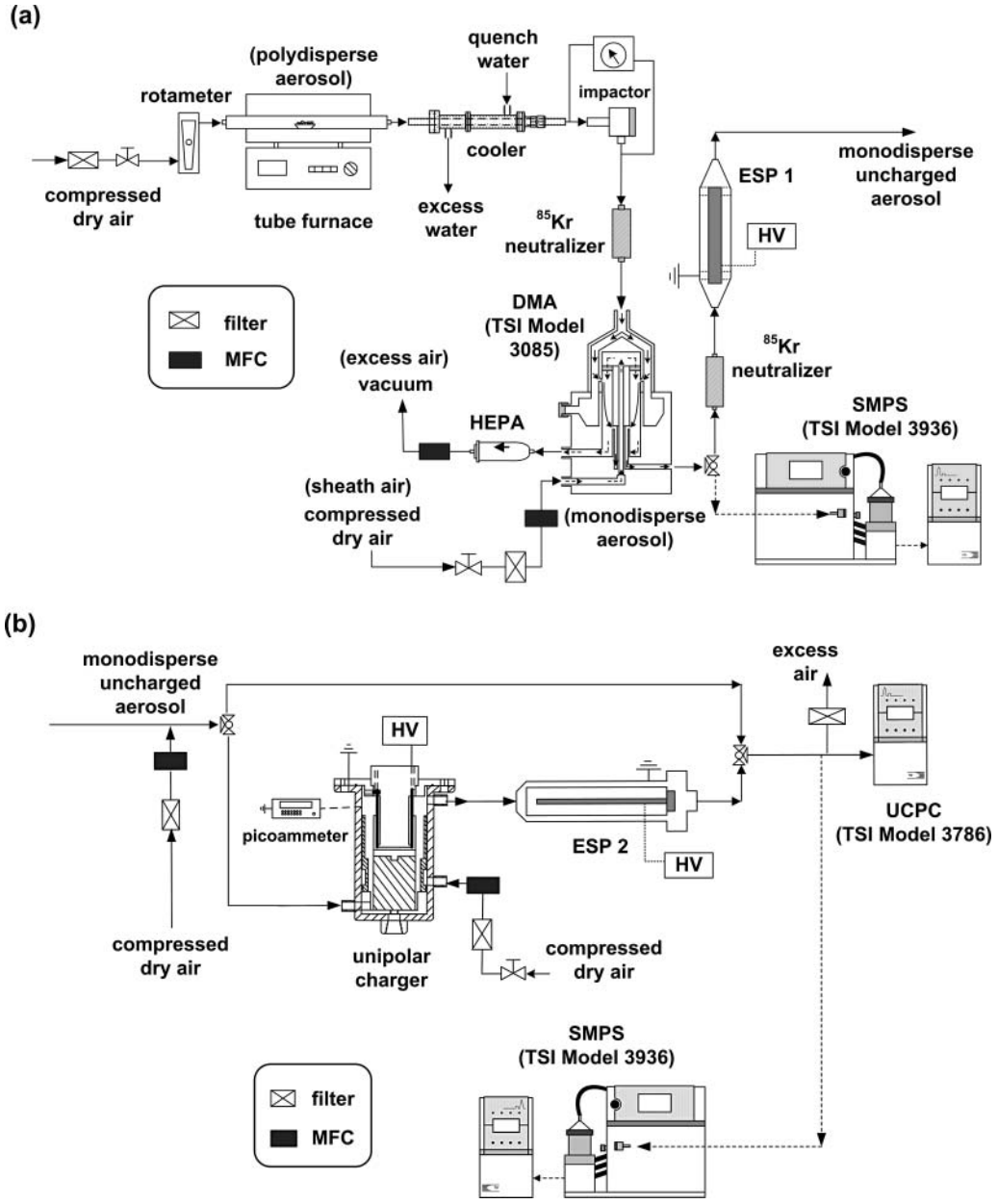

FIG. 2. (a) Schematic diagram of aerosol generation system. (b) Schematic diagram of experimental setup.

Experimental Setup

Figure 2a shows the schematic diagram of the generation system used for producing different sizes of particles in the laboratory. Monodisperse NaCl and Ag nanoparticles with electrical mobility diameter less than 50 nm were generated by the evaporation-condensation technique (Scheibel and Porstendorfer 1983). The material (silver or sodium chloride) of the test aerosols was loaded in a combustion boat placed in a tube furnace. A stream containing vapor of the material was formed by passing clean low-temperature air through the ceramic tube in furnace. Polydisperse nanoparticles of high concentration were produced by quenching the hot stream with passing through a water-based cooler. The particles were neutralized by an ^{85}Kr electrostatic neutralizer (TSI model 3077A), and classified in the Nano-differential mobility analyzer (Nano-DMA, TSI model 3085). The singly charged monodisperse particles were classified from Nano-DMA, then, passed through the second ^{85}Kr neutralizer and an electrostatic precipitator (ESP) to remove charged particles entirely. The uncharged monodisperse test particles were obtained downstream from ESP. Only uncharged particles were introduced into the unipolar chargers.

Figure 2b shows the experimental setup for the evaluation of the chargers. In the charging test system, an additional

Downloaded by [National Chiao Tung University] at 22:44 24 April 2014

compressed filtered air was mixed with uncharged particles to increase the aerosol flow rate to 10 L/min before entering the charger. In the charging zone, a sheath air flow could be introduced from the 0.1 mm or 0.5 mm annular slit along the inner wall of the charger. After charged aerosol flow exited outside the charger, it passed through the second ESP. The charged aerosol flow was further introduced into an ultrafine condensation particle counter (UCPC, TSI model 3786) to measure particle concentration downstream of the charger. When DC voltage is applied, the stainless steel casing was connected to a picoammeter (Keithley Model 6485) which is grounded to measure the corona current. The corona current I versus the corona voltage V could be therefore measured. Due to the low concentration of monodisperse particle which the size is less than 3 nm, we used polydisperse uncharged particle ranged from 2.5 to 3.5 nm as an alternative method to evaluate the charging performance of the charger for 2.5 and 3 nm particles measured by a SMPS.

In this study, both charging efficiencies and losses of unipolar charger with multiple discharging wires were measured. There are four indexes used for evaluating the charging performance of unipolar chargers, including intrinsic charging efficiency (η_{int}), extrinsic charging efficiency(η_{ext}), electrostatic loss (L_{el}), and diffusion loss (L_d^0), which are calculated by the expressions described similar to the criteria of Marquard et al. (2006b), the intrinsic charging efficiency can be computed as:

$$\eta_{\text{int}} = \frac{f}{P_{\text{ESP}}} \frac{C_{\text{out,OFF}} - C_{\text{out}}^0}{C_{\text{in}}} \quad [1]$$

where the dilution factor f is equal to the ratio of the outlet total flow rate to the inlet aerosol flow rates of the charger, P_{ESP} is the penetration of uncharged particles through the second ESP, C_{in} is the particle number concentration counted upstream of the chargers, $C_{\text{out,OFF}}$ is the particle number concentration measured downstream of the charger when no voltage is applied on the charger and the second ESP, C_{out}^0 is the particle number concentration counted downstream of the charger when the charger is on and sufficiently high voltage is applied on the second ESP to remove all charged particles.

The extrinsic charging efficiency, which is the parameter of interest in a practical application, is defined as the fraction of particles exit outside the charger carrying at least a unit of charge, and described as:

$$\eta_{\text{ext}} = \frac{f}{P_{ESP}} \frac{C_{\text{out,ON}} - C_{\text{out}}^0}{C_{\text{in}}} \quad [2]$$

where $C_{\text{out,ON}}$ is the particle number concentration measured downstream of the charger when the charger and the second ESP are on and off, respectively.

Experimental results regarding electrostatic loss and diffusion loss inside the chargers can be calculated by the following equations:

$$L_{\text{el}} = \frac{f}{P_{\text{ESP}}} \frac{C_{\text{out,OFF}} - C_{\text{out,ON}}}{C_{\text{in}}} \quad [3]$$

$$L_d^0 = 1 - \frac{f}{P_{\text{ESP}}} \frac{C_{\text{out,OFF}}}{C_{\text{in}}} \quad [4]$$

Measurement of Particle Charge Distribution

The tandem-DMA method was used to measure the charge distribution of monodisperse particles of different sizes. As shown in Figure 2b, it is similar to Alguacil and Alonso (2006). When monodisperse particles were charged in the unipolar charger, SMPS without ^{85}Kr neutralizer installed was used to scan the size distribution of the charged particles at the exit of the charger. The scanning distributions maybe contain multiple modes appearing at mobility values which represent the mobility of different multiple charged particles at the same size. When applying different corona voltages, there's a corresponding charge distribution of charged particles. Each mode on the scanning diagram is a specific number of elementary charges per particle. The relative fractions of multiply charged particles are determined from the relative areas under their corresponding peaks, called "charge distribution in the exit" (Marquard et al. 2006b), it means the charge distribution is not in the charging zone due to the charged particle loss exists.

RESULTS AND DISCUSSION

Nanoparticle Concentration

In this study, nano-sized sodium chloride and silver particles generated by the evaporation-condensation technique were classified in the Nano-DMA to produce monodisperse particles. The performance of the charger with multiple discharging wires was tested by using the monodisperse sodium chloride particles of 10 $\sim$ 50 nm and silver particles of 2.5 $\sim$ 10 nm in diameter. Figures 3a and b plot the generated nanoparticle concentration and size distribution for sodium chloride and silver particles, respectively. Results show that the concentrations of sodium chloride and silver particles range from 1×10^2 to 1×10^8 #/cm^3 for the various furnace temperatures at the carry flow rate of 1 L/min.

Relationship between Ion Current and Corona Voltage

The $N_i t$ product is a basic index to describe the operation of a corona aerosol charger; it is the key parameter in charging by ion diffusion mechanism. A greater $N_i t$ product would make sure of the higher intrinsic charging efficiency. The corona current, I, varied as applied voltage was measured, and the ion concentration N_i was assumed to be related to the corona current. N_i

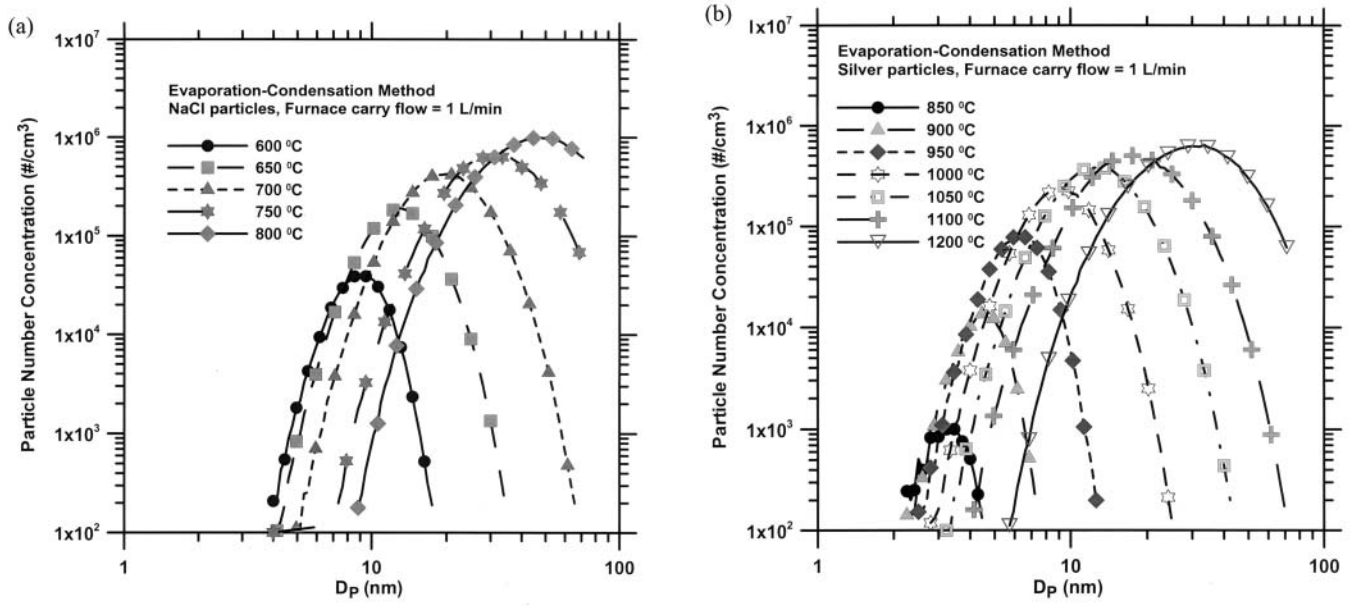

FIG. 3. Nanoparticle concentration and size distribution (a) sodium chloride particles (b) silver particles.

values can be estimated by following equation:

$$N_i = \frac{I \ln\left(r_2/r_1\right)}{2\pi V Z_i L e} \quad [5]$$

where r_1 is the radius of the discharging wires, r_2 is the distance between the outer casing and discharging wires, Z_i is the electrical mobility of positive ions (1.4×10^{-4} m^2/V-sec), L is the effective length of the discharging wires, and e is the elementary charge (1.6×10^{-19} C).

As shown in Figure 4, the ion current was found as a function of applied positive voltage for the charger at the aerosol flow rate of 10 L/min. When the positive corona voltage increases from + 4.0 kV to +10 kV, the corona current will increase from 0.02 to 119.63 μA and the ion concentration will increase from 1.9×10^7 to 3.9×10^{10} ions/cm^3. The residence time in the charging zone is 0.136 to 0.045 s when the sheath flow rate is from 0 to 20 L/min at the aerosol flow rate of 10 L/min. The ion concentration in the charging zone can be controlled by the corona current or the corona voltage. That is, an increasing corona voltage can lead to a higher corona current; more ions were therefore generated from the surface of the corona wire. It results in the possibility of an increasing intrinsic charging efficiency of the unipolar charger with multiple discharging wires.

Intrinsic Charging Efficiency

In present study, the intrinsic charging efficiency was investigated at different sheath flow rates, corona voltages, and mean velocities of sheath air. Figure 5 shows the intrinsic charging efficiency of the charger with multiple discharging wires for 10 nm silver particles at various sheath flow rates and corona voltages. The test aerosol flow rate was fixed at 10 L/min. For the case of no sheath air used in the charger, the intrinsic charging efficiency is larger than those of 10 and 20 L/min sheath flow rate at the same voltage. The intrinsic charging efficiency decreases with increasing sheath air flow rate, because of the shorter residence time of the particles in the charging zone for the larger sheath flow rate. In addition, the intrinsic charging efficiency of no sheath air at +6.4 kV is close to that of 20 L/min sheath

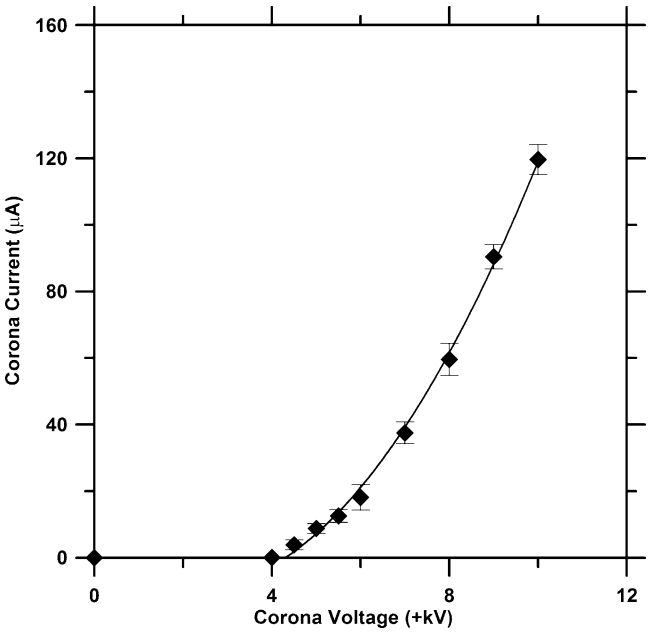

FIG. 4. Corona current vs. corona voltage inside charger.

Downloaded by [National Chiao Tung University] at 22:44 24 April 2014

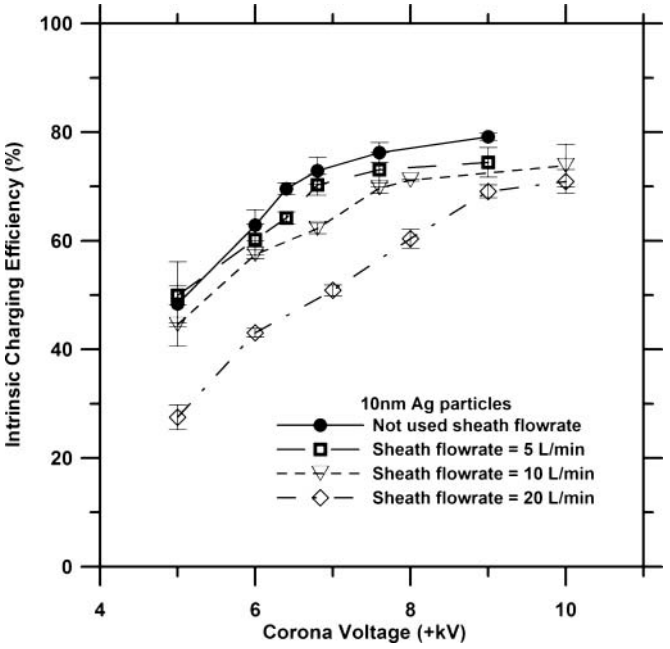

FIG. 5. Intrinsic charging efficiency as a function of corona voltage.

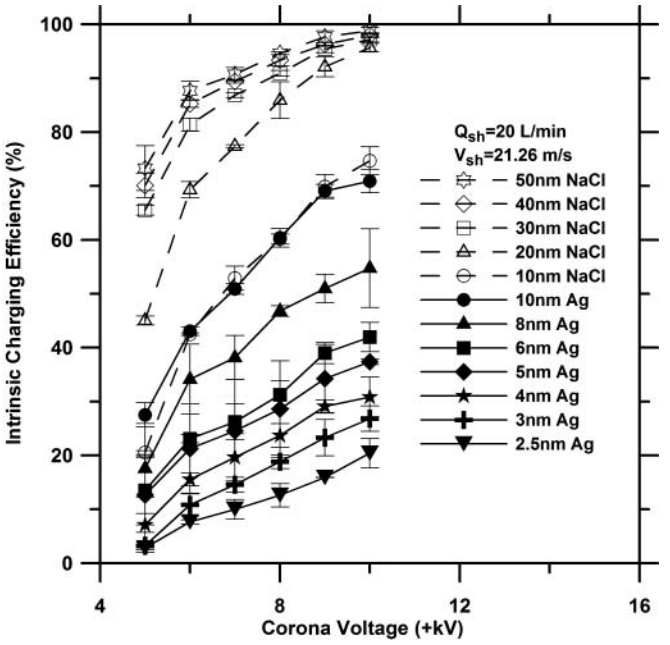

FIG. 7. Intrinsic charging efficiency as a function of corona voltage.

air at +9 kV for 10 nm silver particles. Figure 6 shows the intrinsic charging efficiency of the charger with multiple discharging wires at the various particle sizes and mean velocities. It demonstrates that a higher mean velocity of the sheath air would get particles easily away from the charging zone, so that the intrinsic charging efficiency will be slightly decreased.

Figure 7 shows the intrinsic charging efficiency of the particles which size ranged from 2.5 to 50 nm for the different applied voltages at the sheath flow rate of 20 L/min. Results show that the intrinsic charging efficiencies increase with increasing the corona voltages and particle sizes. However, the intrinsic charging efficiency can only display a part of performance of the charger. It is necessary to optimize the performance of the charger and to find out the optimal operating condition.

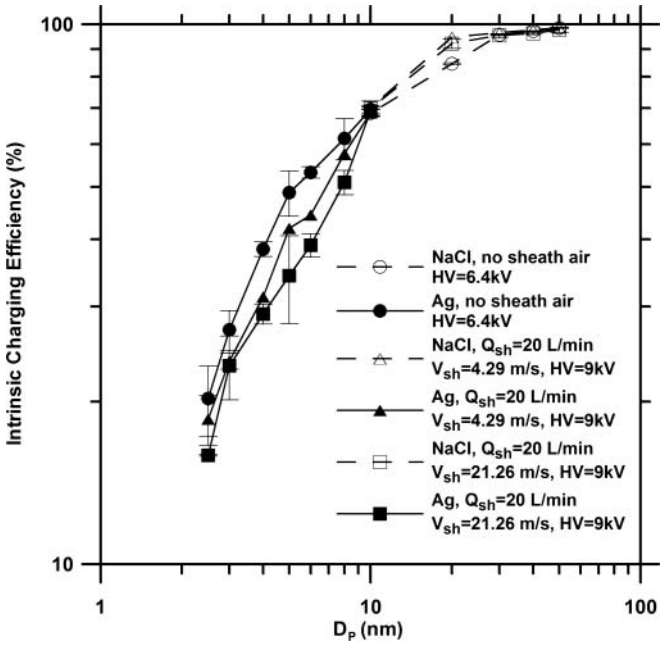

FIG. 6. Intrinsic charging efficiency as a function of particle size.

Electrostatic Loss and Diffusion Loss

When the corona voltages are increased to raise the fraction of charged particles and the intrinsic charging efficiencies, it's important to let the charged particles pass through the charger. The fraction of particle loss also needs to be reduced. As seen in Figure 8, the electrostatic loss of charged particles due to the deposition by the electrical field and space charge exists in the charger at different sheath air flow rates and corona voltages. It is evident that an increase in the sheath air flow rate decreases the electrostatic loss of charged particles at the same applied voltage in the charger. It is because that the sheath air flow can carry the charged particles fast through the charging zone, preventing the charged particles from deposited by the strong electrical field.

Figure 9 shows the electrostatic loss of charged particles ranged from 2.5 to 50 nm in particle sizes at different mean velocities of sheath air flow in the charger. The most electrostatic loss is seen to occur at 10 nm charged particles. It is due to the charged fraction of the particles less than 10 nm decreases with decreasing particle diameter, on the other hand, the electrical mobility of the particles greater than 10 nm lessens as the particle size increased. The electrostatic loss of the charged particles in the charger at other sheath air velocities was found to have the

Downloaded by [National Chiao Tung University] at 22:44 24 April 2014

Downloaded by [National Chiao Tung University] at 22:44 24 April 2014

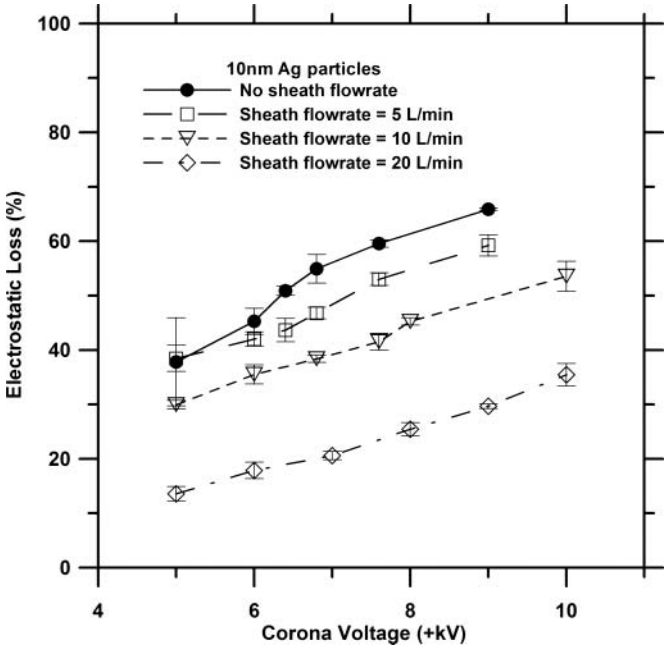

FIG. 8. Electrostatic loss as a function of corona voltage.

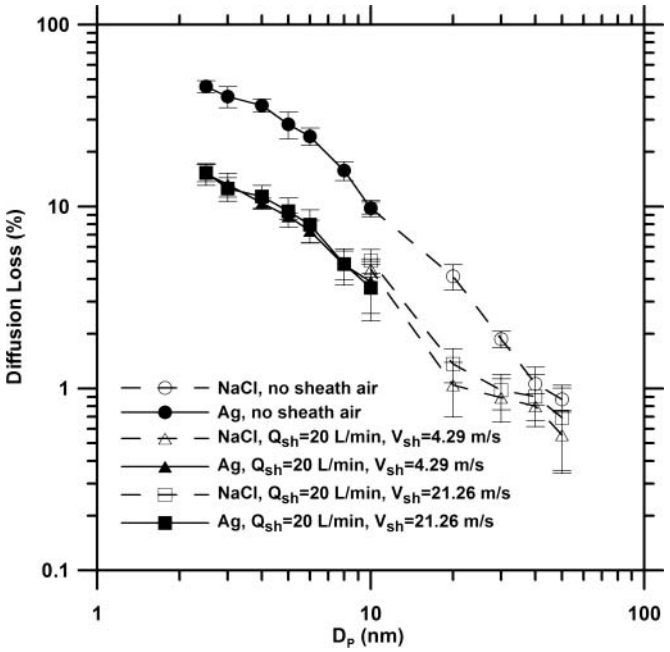

FIG. 10. Diffusion loss as a function of particle size.

similar results. Moreover, the higher mean velocity of sheath air flow can slightly reduce the electrostatic loss of the charged particles.

Figure 10 shows the diffusion loss of uncharged particles in the charger at different mean velocities of sheath air flow and particle sizes. Compared to the case without sheath air flow, the diffusion loss of uncharged particles is smaller for the sheath air flow of 20 L/min, due to the shorter residence time in the charger. For the case of higher mean velocity of sheath air flow, the diffusion loss of particle size ranged from 2.5 to 50 nm is close to that of lower mean velocity of sheath air flow.

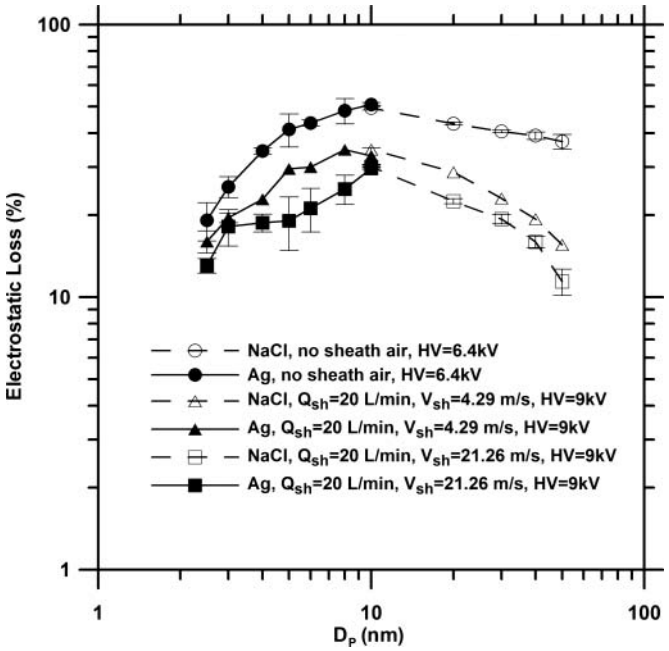

FIG. 9. Electrostatic loss as a function of particle size.

Extrinsic Charging Efficiency

Compared with the intrinsic charging efficiency, the extrinsic charging efficiency of the charger with multiple discharging wires is more significant with practice. The extrinsic charging efficiency represents the capability of the charger to offer charged particles, so it is frequently used to optimize the performance of the charger. As shown in Figure 11, it is the extrinsic charging efficiency for 10 nm particles in the charger at the different sheath air flow rates and corona voltages. There is an optimal extrinsic charging efficiency for the different corona voltages at each sheath air flow rate in the charger. In general, the extrinsic charging efficiencies of 10 nm particles increase with increasing the sheath flow rate at various corona voltages. The highest extrinsic charging efficiency for 10 nm particles is 39.4% at sheath air flow rate of 20 L/min and applied voltage of +9 kV.

Figure 12 shows the extrinsic charging efficiency of the particles ranged from 2.5 to 50 nm for various mean velocities of sheath air flow at the optimal applied voltage. A higher mean velocity of sheath air flow can slightly enhance the extrinsic charging efficiency at the same sheath air flow rate; it is because those charged particles are easier to pass through the charging zone near the wall of the charger.

Figure 13 shows the extrinsic charging efficiency of the particles ranged from 2.5 to 50 nm for the different applied voltages at

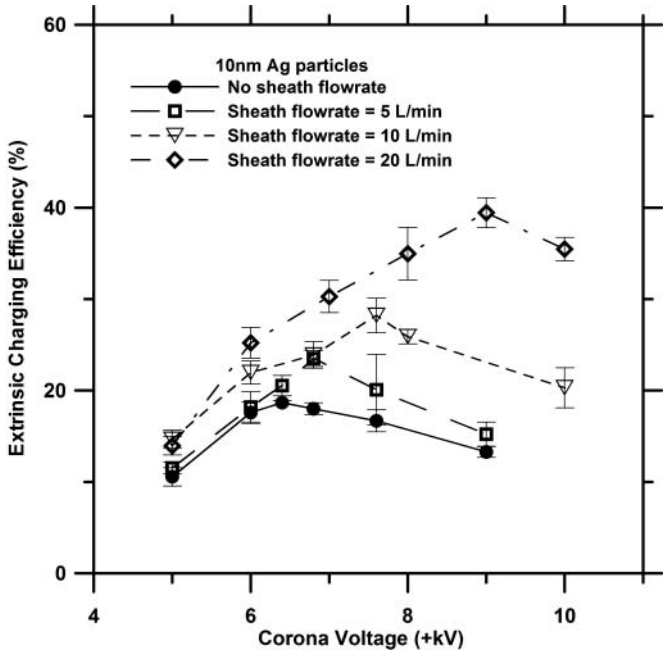

FIG. 11. Extrinsic charging efficiency as a function of corona voltage.

the sheath flow rate of 20 L/min. Results show that the extrinsic charging efficiency increases as the particle size increases. In addition, the higher extrinsic charging efficiency can be obtained with a sufficiently high discharging voltage at an appropriate sheath air flow rate and mean sheath air velocity. The best extrinsic charging efficiency of 2.86–86.3% for particles ranging from 2.5 to 50 nm is seen to occur at +9.0 kV in the charger with multiple discharging wires.

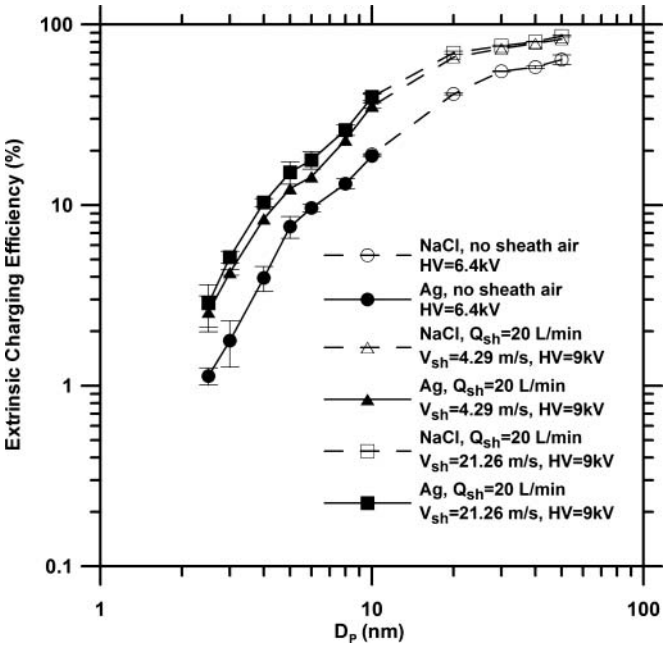

FIG. 12. Extrinsic charging efficiency as a function of particle size.

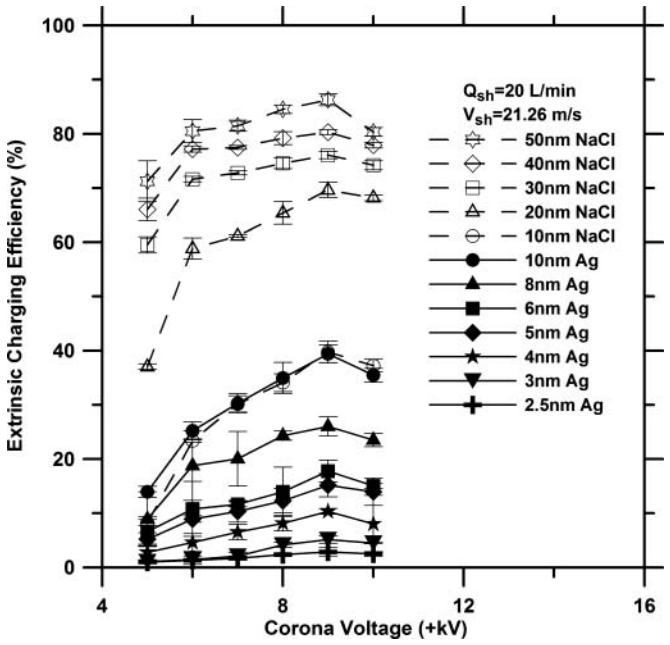

FIG. 13. Extrinsic charging efficiency as a function of corona voltage.

The maximum extrinsic charging efficiency was compared with those of previous chargers, as shown in Figure 14. It is seen that the extrinsic charging efficiencies of present charger with sheath air operating at 20 L/min sheath air flow rate and +9 kV applied voltage are higher than the other chargers which have no sheath air for particles less than 10 nm. For the charger

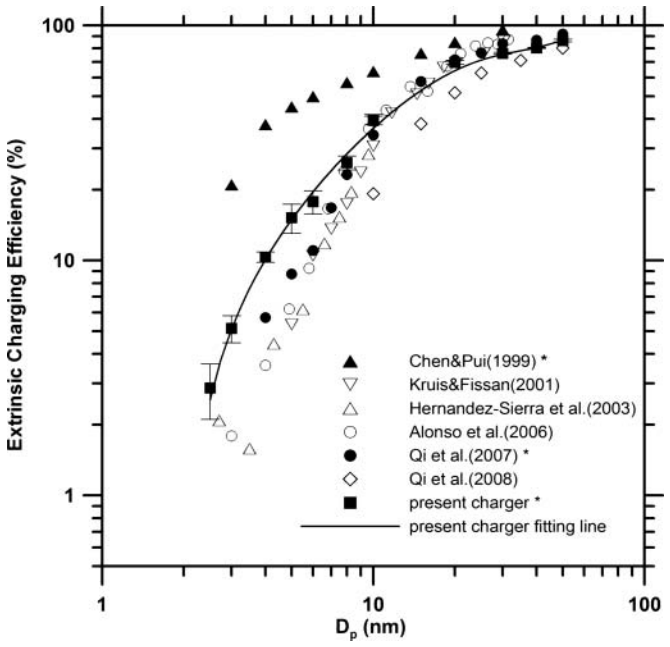

FIG. 14. Comparison of the extrinsic charging efficiency of present charger with the previous data in other researches as a function of particle size (charger with sheath air: *Chen & Pui (1999), *Qi et al. (2007), and *present charger. The other chargers have no sheath air).

Downloaded by [National Chiao Tung University] at 22:44 24 April 2014

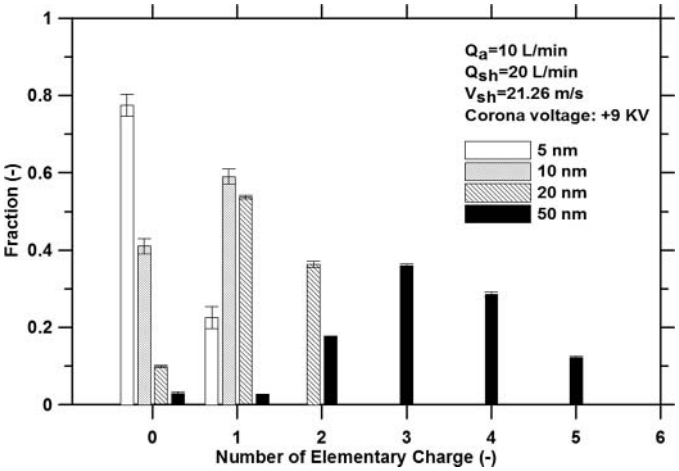

FIG. 15. Charge distribution in the exit of charger as a function of particle diameter. The aerosol flow rate and sheath air flow rate are 10 L/min and 20 L/min, respectively. The operating voltage is +9 kV.

with sheath air, the results show that the extrinsic charging efficiencies of present charger are higher than those of Qi et al. (2007); but are lower than those of Chen and Pui (1999). However, this study demonstrates that the charger operating at 20 L/min sheath air flow rate and +9 kV applied voltage has the optimal extrinsic charging efficiency. Moreover, compared to the previous results (Tsai et al. 2008), the present charger with sheath air has lower particle losses. For example, there are about 30% electrostatic loss and 5% diffusion loss for 10 nm particles, and electrostatic loss of 19% and diffusion loss of 9.4% for particles of 5 nm in the charger. Therefore, it is efficient to reduce the particle loss by using the sheath air flow rate at an appropriate discharging voltage to enhance the extrinsic charging efficiency of the charger with multiple discharging wires.

Measured Particle Charge Distribution

Beside the extrinsic charging efficiency, the charge distribution of particles passing through the charger with multiple discharging wires is necessary to obtain for many practical applications. In this study, the charge distributions in the exit of the charger for the particles with different sizes were measured. Figure 15 shows the charge distribution for the particles of 5, 10, 20, and 50 nm in the exit of the charger at 20 L/min sheath flow rate and +9 kV applied voltage. The results demonstrate that the particles are singly charged or uncharged for the particle diameter smaller than 10 nm. For larger particles, the fraction of multiply charged particles is found to be higher. Some fraction of particles carrying five charges was observed for particles in 50 nm diameter.

CONCLUSIONS

A unipolar charger with multiple discharging wires has been developed and investigated to enhance the extrinsic charging efficiency of nanopartricles by using sheath air near the wall of the charger to reduce the electrostatic loss of nanoparticles. The charging performance of the charger was carried out under different operating conditions including sheath flow rates, corona voltages, and mean velocities of sheath air flow for particles ranging from 2.5 to 50 nm. The applied voltage of the charger ranged from $+4.0 \sim +10$ kV, corresponding to corona current from 0.02 to 119.63 μA. Increasing the corona voltage can lead to a higher corona current, with more ions generated, leading to an increase in the intrinsic charging efficiency. However, the higher electrostatic loss occurred due to a stronger electrical field. By shortening the residence time in the charging region by increasing the sheath flow from $5 \sim 20$ L/min, the extrinsic charging efficiency was found to vary with the optimal value obtained at 20 L/min. The mean velocity of sheath air flow near the tube wall slightly enhanced the extrinsic charging efficiency by reducing little electrostatic loss. The optimal operational condition for particles of $2.5 \sim 50$ nm in diameter with the highest extrinsic charging efficiency of $2.86 \sim 86.3\%$ in the charger was obtained at +9 kV corona voltage, 10 L/min aerosol flow, and 20 L/min sheath air flow. The TDMA technique was further utilized to analyze the charge distribution in the exit of particles. The results show that the particles are singly charged or uncharged for diameter smaller than 10 nm. For particles larger than 20 nm, the fraction of multiply charged particles becomes higher.

NOMENCLATURE

C_{in}	particle number concentration upstream of charger
C^0_{out}	particle number concentration downstream of charger (charger on; second ESP on)
$C_{out,OFF}$	particle number concentration downstream of charger (charger off; second ESP off)
$C_{out,ON}$	particle number concentration downstream of charger (charger on; second ESP off)
e	elementary charge
f	dilution factor
I	corona current
L	effective length of discharging wire
L_{el}	electrostatic loss inside charger
L^0_d	diffusion loss inside charger
N_i	ion concentration
P_{ESP}	penetration of uncharged particles through second ESP
Q_{sh}	sheath air flow rate
V_{sh}	sheath air velocity
r_1	radius of discharging wire
r_2	distance between outer casing and discharging wire
V	applied voltage
Z_i	electrical mobility of positive ions
η_{int}	intrinsic charging efficiency
η_{ext}	extrinsic charging efficiency

REFERENCES

Alguacil, F. J., and Alonso, M. (2006). Multiple Charging of Ultrafine Particles in a Corona Charger. *J. Aerosol Sci.* 37:875–884.

Downloaded by [National Chiao Tung University] at 22:44 24 April 2014

Alonso, M., Martin, M. I., and Alguacil, F. J. (2006). The Measurement of Charging Efficiencies and Losses of Nanoparticles in a Corona Charger. *J. Electrostatics* 64:203–214.

Biskos, G., Reavell, K., and Collings, N. (2005). Unipolar Diffusion Charging of Aerosol Particles in the Transition Regime. *J. Electrostatics* 36:247–265.

Buscher, P., Schmidt-Ott, A., and Wiedensohler, A. (1994). Performance of a Unipolar "Square Wave" Diffusion Charger with Variable nt-Product. *J. Aerosol Sci.* 25:651–663.

Chen, D. R., and Pui, D. Y. H. (1999). A High Efficiency, High Throughput Unipolar Aerosol Charger for Nanoparticles. *J. Nanoparticle Res.* 1:115–126.

Hernandez-Sierra, A., Alguacil, F. J., and Alonso, M. (2003). Unipolar Charging of Nanometer Aerosol Particles in a Corona Ionizer. *J. Aerosol Sci.* 34:733–745.

Huang, S. H., and Chen, C. C. (2002). Ultrafine Aerosol Penetration through Electrostatic Precipitator. *Environ. Sci. Technol.* 36:4625–4632.

Kruis, F. E., and Fissan, H. (2001). Nanoparticle Charging in a Twin Hewitt Charger. *J. Nanoparticle Res.* 3:39–50.

Knutson, E. O., and Witby, K. T. (1975). Aerosol Classification by Electric Mobility: Apparatus, Theory, and Applications. *J. Aerosol Sci.* 6:443–451.

Marquard, A., Meyer, J., and Kasper, G. (2006a). Characterization of Unipolar Electrical Aerosol Chargers—Part II: Application of Comparison Criteria to Various Types of Nanoaerosol Charging Devices. *J. Aerosol Sci.* 37:1069–1080.

Marquard, M., Meyer, J., and Kasper, G. (2006b). Characterization of Unipolar Electrical Aerosol Chargers—Part I: A Review of Charger Performance Criteria. *J. Aerosol Sci.* 37:1052–1068.

Qi, C., Chen, D. R., and Greenberg, P. (2008). Performance Study of a Unipolar Minicharger for a Personal Nanoparticle Sizer. *J. Aerosol Sci.* 39:450–459.

Qi, C., Chen, D. R., and Pui, D. Y. H. (2007). Experimental Study of a New Corona–Based Unipolar Aerosol Charger. *J. Aerosol Sci.* 38:775–792.

Reischl, G.. P., Mäkelä, J. M., and Necid, J. (1996). Bipolar Charging of Ultrafine Particles in the Size Range Below 10nm. *J. Aerosol Sci.* 27:931–949.

Scheibel, H.-G., and Porstendorfer, J. (1983). Generation of Monodisperse Ag- and NaCl-Aerosol with Particle Diameters Between 2 and 300 nm. *J. Aerosol Sci.* 14:113–126.

Tsai, C.-J., Chen, S. C., Chen, H.-L., Chein, H. M., Wu, C.-H., and Chen, T. M. (2008). Study of a Nanoparticle Charger Containing Multiple Discharging Wires in a Tube. *Sep. Sci. Technol.* 43:3476–3493.

Wang, S. C., and Flagan, R. C. (1990). Scanning Electrical Mobility Spectrometer. *Aerosol Sci. Technol.* 13:230–240.

Wiedensohler, A., Buscher, P., Hansson, H. C., Martinsson, B. G., Stratmann, F., Ferron, G., and Busch, B. (1994). A Novel Unipolar Charger for Ultrafine Aerosol Particles with Minimal Particle Losses. *J. Aerosol Sci.* 25: 639–649.

Yoo, K. H., Lee, J. S., and Oh, M. D. (1997). Charging Collection of Submicron Particles in Two-Stage Parallel-Plate Electrostatic Precipitators. *Aerosol Sci. Technol.* 27:308–323.

Downloaded by [National Chiao Tung University] at 22:44 24 April 2014